Electrochemically induced bulk nanobubbles

Jadhav, Anand; Barigou, Mostafa

DOI:
10.1021/acs.iecr.1c04046

Document Version
Peer reviewed version

Citation for published version (Harvard):
Jadhav, A & Barigou, M 2021, 'Electrochemically induced bulk nanobubbles', *Industrial & Engineering Chemistry Research*, vol. 60, no. 49, pp. 17999-18006. https://doi.org/10.1021/acs.iecr.1c04046

Electrochemically induced bulk nanobubbles

Ananda J. Jadhav, Mostafa Barigou*

School of Chemical Engineering, University of Birmingham, Edgbaston, Birmingham B15 2TT, United Kingdom

Abstract

We describe the generation of bulk nanobubbles using electrolysis of aqueous alkaline, neutral or acidic electrolytes. The technique can be used in either an undivided electrolytic cell to generate a mixture of bulk nanobubbles filled with different gases, for example, a hydrogen- and oxygen-filled bulk nanobubble suspension, or in a divided electrolytic cell to prepare separate hydrogen- and oxygen-filled bulk nanobubble suspensions. We systematically study the effects of the operating parameters on the characteristics of the nanobubbles formed and the effectiveness of their generation. A greater current input, longer operating time, higher electrolyte concentration or lower water operating temperature enhance the production of nanobubbles. The type of electrolyte determines the colloidal stability of the nanobubbles formed. In all types of electrolyte solutions, the initial bubble size is on the order of 100 nm. Bulk nanobubbles in an alkaline electrolyte exist in a stable cluster form, but they dissociate into tiny primary nanobubbles on the order of 1 nm in neutral and acidic electrolytes, which is consistent with our previous findings on the clustering of bulk nanobubbles.

*Corresponding author; Email: m.barigou@bham.ac.uk

1. Introduction

The ever increasing interest in the emerging field of bulk nanobubbles (BNBs) sometimes also referred to as ultrafine bubbles,[1] has led to the exploration of diverse techniques for their production including. We recently summarised the state-of-the art and discussed the major advances in this area.[2] The main BNB generation methods proposed to date include high-shear rotor-stator devices operating in batch or continuous mode,[2] microfluidics,[3,4] water-solvent mixing,[5–8] hydrodynamic cavitation,[9–21] acoustic cavitation,[3,5,22,23] periodic pressure change method,[24] pressure induced supersaturation,[25] and nano-membranes.[26–29] A review of the relevant literature shows, however, that there is still a need for new efficient BNB production methods to fulfil the requirements of the diverse industrial applications which are anticipated. Ideally, such techniques should be 'clean', not prone to impurities and contamination, should be amenable to process control and able to yield high concentrations of BNBs on large scales and at reduced costs.

Electrolysis of water has traditionally been used for the production of hydrogen for commercial applications[30] and has been the subject of extensive studies. The passing of a direct electric current through an electrolyte solution induces a reduction reaction occurring at the cathode which causes the release of H_2 gas molecules. Similarly, oxidation of the hydroxyl group OH^- results in the formation of O_2 gas molecules. Such a technique, therefore, seems to be a good candidate for producing microbubbles and nanobubbles. Furthermore, it has the potential to impact a number of technologies including, for instance, fuel cell technology as the high pressure inside nanobubbles should increase gas reactivity which makes them potentially useful catalysts-free reactors; for example, O_2 and H_2 nanobubbles could be used as reactants in a fuel cell to replace expensive and heavy catalysts.[31] Indeed, it has been reported that both bulk[32–34] and surface nanobubbles[35] of hydrogen and oxygen gas can be generated by electrolysis of water in an electrochemical cell. These reports are, however, limited in both number and scope and have not addressed the fundamental and operational aspects of the electrolysis process for BNB generation. Therefore, systematic investigations of the various pertinent parameters such as ionic strength, strength of electric field and type of electrode surface, are needed to optimize the number concentration and size of the nanobubbles, thus, produced.

In this paper, we study in detail a method for generating BNB suspensions in alkaline, neutral and acidic electrolyte solutions, based on the principle of electrolysis. We explore the technique in batch mode and in continuous mode, and systematically investigate the role of various operating parameters including the type of electrolyte and its concentration, applied voltage, operating time and temperature, and identify conditions for optimising BNB production.

2. Materials and methods

2.1 Materials

All experiments used ultrapure water (type-1) provided by a Millipore station (Avidity Science, UK). The pH and conductivity of the ultrapure water (henceforward referred to simply as pure water) measured at a temperature of 20 ˚C were 6.7 and 0.055 $\mu S.cm^{-1}$, respectively. Furthermore, only the purest reagents and solvents available commercially were employed. Analytical grade (99.9% pure, Sigma Aldrich, UK) reagents were used to make the stock solutions of potassium hydroxide (KOH), sodium chloride (NaCl) and hydrochloric acid (HCL). Such solutions were prepared and stored using glassware to avoid the possibility of contamination that may arise from the use of plasticware. Cleaning of all glassware consisted of three consecutive steps: (i) immersion for 30 min in a 10% aqueous solution of potassium hydroxide assisted by ultrasound irradiation in an ultrasound bath; (ii) rinsing with copious amounts of pure water; and (iii) thorough drying using a combination of dry-air jet impingement and microwave oven drying. The dry air used was obtained from BOC (UK) and had a purity >99.5%. Similarly, the electrodes of the electrochemical cell were subjected to copious rinsing with pure water and flushed with a jet of dry air. Experiments to produce BNBs were preceded by analysis of the pure water and stock solutions by means of a Nanosight instrument to confirm the absence of any significant amounts of nanoscale impurities. The Nanosight instrument was also utilised to measure the size distribution of the BNBs and their bubble number density, as described further below. Once formed, the BNB suspensions were collected from the electrochemical cell and kept in 20 mL air-tight glass vials for subequent analysis.

2.2 Methods of BNB generation

Experiments to generate BNB suspensions were conducted using both a batch electrolysis system (BES) and a continuous electrolysis system (CES), as follows.

2.2.1 Batch electrolysis system (BES)

The batch electrolysis process was conducted in a 250 mL jacketed glass vessel, as schematically represented in Figure 1. Temperature control to within ± 1 °C was achieved using an external recirculating cooler (JULABO GmbH, Germany). An undivided electrolytic cell (Baoji Ruicheng Titanium Industry Co. Ltd, China) with six platinum-coated titanium-plate electrodes (10 cm × 6 cm × 0.1 cm) was used. The electrodes were positioned vertically in parallel with an inter-electrode gap of 2 cm, and were fed by a DC power supply (Eventek, 0-30V, 0-10A, China). Electrolysis experiments were run under various conditions of alkaline, acidic and neutral electrolyte solutions of different concentrations, for different values of applied voltage, operating time and temperature.

2.2.2 Continuous electrolysis system (CES)

A laboratory-scale electrochemical flow cell (C-Tech Innovation Ltd.) was used to produce BNBs in an aqueous alkaline salt solution. The configuration and components of the electrochemical flow cell are depicted in Figure 2. The cell has an active electrode area of 25 cm^2 and a net half-cell working volume of 12.5 cm^3 (i.e. a total volume of 25 cm^3 not including the separation membrane). The cell is divided in two halves separated by a proton exchange membrane Nafion 212 (Alfa Aesar, UK), having a dry thickness of 0.05 mm. The whole cell unit is contained between two stainless steel endplates. The electrolyte solution is fed into the cell through the bottom inlet manifold; it branches into two separate streams through the ports, flows through the electrode compartment and exits through the top outlet manifold. The outflows from the two branches are collected in separate vials for further analysis. A more detailed description of this electrochemical flow cell can be found on the manufacturer's website.[36]

2.3 Characterisation of BNB suspensions

Under different operating conditions, the electrolysis process generated distributions of BNB sizes which had very different spreads. Given the wide spectrum of BNB sizes encountered, it was necessary to use two different complementary techniques namely, nanoparticle tracking analysis (NTA) and dynamic laser scattering (DLS), to characterise the various BNB suspensions obtained.

2.3.1 NTA technique

NTA has bcome a popular technique for analysing nanoparticle suspensions, including BNB suspensions. It relies on tracking the Brownian motion of nano-entities in a liquid and using their light scattering effects to infer their size distribution. The method is suitable for the analysis of polydisperse mixtures in real time having particle concentrations ranging from 10^7 to 10^9 particles.mL^{-1} and particle sizes ranging from 10 to 2000 nm. It has the added advantage of being able to determine the number density of the suspended nano-entities observed. In this study, we used a NanoSight NS300 instrument (Malvern-UK) for the characterisation of BNB suspensions which fell within its operating particle size range. We have made extensive use of this technique in our previous studies and discussed its merits as well as its shortcomings compared to the DLS technique, as summarised below.[3,37,38]

2.3.2 DLS technique

DLS is another well-established technique which can measure nanoparticle size distributions from 0.3 nm to 10 μm, i.e. over a much wider range than NTA. It can also handle particle concentrations from 10^8 to 10^{12} particles.mL^{-1}.[39,40] A popular DLS instrument is the ZEN5600 Zetasizer Nano ZSP

(Malvern Instruments) which was used for analysing BNB suspensions in this work. The instrument analyses the light intensity fluctuations arising from laser scattering caused by the Brownian motion of the particles in suspension to determine their velocity. Use of the Einstein–Stokes relationship then leads to an estimation of particle size.[41] Unlike NTA, however, DLS measurements do not yield the particle number density. We also showed previously that DLS tends to overestimate particle size when measuring particles on the order of 10 nm and above.[3] Hence, DLS was employed in this study to complement the NTA method at the lower end of the spectrum, i.e. to measure BNBs on the 1 nm order which NTA cannot resolve. The DLS instrument has the additional advantage of being able to measure the zeta potential of BNBs, which is useful for characterising their stability. Both the NTA and DLS instruments were routinely checked to ascertain their consistent accuracy and precision by analysing standard suspensions of monosize latex nanospheres, and enable the fine tuning of their various settings accordingly.

2.3.3 Analysis of impurities and contamination

The BNB suspensions generated in the electrochemical cell were thoroughly analysed for the presence of any impurities or contamination using established techniques and protocols we reported in our previous studies.[3,5] Two different analytical techniques, namely inductive coupled plasma mass spectroscopy (ICPMS) and gas chromatography mass spectroscopy (GCMS), were used to examine the BNB suspensions for any nanoscale metal or organic impurities that might have stemmed from the electrochemical process and which could potentially be construed as BNBs. The ICPMS analsyis showed that the amount of metal impurities was insignificant and not different from what is usually expected in a standard aqueous electrolyte solution. Likewise, GCMS revealed a mass spectrum identical to that of an aqueous electrolyte solution, confirming the absence of any signficant nansocale organic impurities. Therefore, the electrolysis process was deemed ‘clean’ and not prone to any impurities or contamination.

3 Results and discussion

3.1 Generation of BNBs in the batch electrolysis system

Using the BES cell (Figure 1), BNBs were generated in aqueous solutions of alkaline electrolyte (using KOH), neutral electrolyte (using NaCl) or acidic electrolyte (using HCl) and the operating parameters, as discussed below, were systematically investigated to maximise the bubble number density. The working mechanism of water electrolysis in the presence of either alkaline, neutral or acidic salt, is based on the supersaturation of electrolytic gases, e.g. oxygen and hydrogen at the anode and cathode, respectively, causing bubbles to be nucleated. During electrolysis, a white cloud of microbubbles forms which disappears when the electrolysis stops. The formation of BNBs is

presumed to take place through either or both of two mechanisms: (i) some of the microbubbles may shrink to form BNBs; and/or (ii) the electrolysis process leads directly to the formation of BNBs.

The effects of the type of electrolyte solution (alkaline, neutral, acidic), electrolyte concentration (E_c), operating time (t), operating temperature (T) and applied voltage (ΔV) on the generation of bulk nanobubbles were studied.

3.1.1 Effects of type of electrolyte

The electrolysis was carried out in aqueous alkaline, neutral and acidic electrolyte solutions of concentration 10 mM at an applied voltage of 10V. The operating time and temperature were 60 min and 20 ºC, respectively. The BNB suspension obtained was immediately analysed at the end of the electrolysis (~ 5 min) and after a period of 24 hr. Results in Figure 3 showing the mean bubble diameter and the bubble number density obtained from NTA analysis in each electrolyte solution, confirm that BNBs can form in all types of electrolyte solutions. BNBs in the alkaline solution were stable after 24 hr with no significant change in their bubble number density. However, in the case of neutral and acidic electrolytes the bubble number density dropped drastically to near zero after 24 hr, falling below the resolution limit of the NTA instrument. These results are consistent with our previous findings, in that BNBs seem to disappear at acidic pH and in neutral salt solutions but remain stable and visible at neutral and basic pH.[3,25,37,38] Note that in case of neutral (NaCl) electrolyte there is an extra complication in terms of BNB formation. Chlorine and hydrogen gas forms at the anode and cathode, respectively. Being highly reactive with water, chlorine does not form BNBs, instead it forms hypochlorous acid and HCl, so that only hydrogen-filled BNBs are expected to form in this acidic medium.

We have shown in a recent study, however, that BNBs normally exist in a cluster form in pure water of neutral or alkaline pH.[38] Thus, the BNBs observed here in the NTA instrument (order 100 nm) are in fact clusters of much smaller primary nanobubbles. In acidic media or in the presence of small amounts of salt, the BNB clusters dissociate into tiny primary nanobubbles on the order of 1 nm. Such primary nanobubbles are stable but are below the resolution limit of the NTA instrument and cannot be detected by this method. They can, however, be resolved by the DLS method, as shown Figure 4. Given that the BNB clusters produced in the neutral and acidic electrolyte solutions were not stable, the detailed study of the effects of the various operating parameters, as discussed below, was entirely focused on electrolysis in alkaline electrolytes, based on NTA analysis.

3.1.2 Effects of operating time

Using the BES cell, electrolysis was carried out for different operating times at a constant applied voltage of 10V in an aqueous alkaline electrolyte of concentration 10 mM, at a temperature of 20 °C. The effects are depicted in Figure 5. The operating time has little effect on the mean diameter and zeta potential of the BNBs formed. The bubble number density, however, increases exponentially with operating time. For a constant applied voltage, the ionic flux increases with time enhancing oxidation and reduction of electrolyte, respectively, on the anode and the cathode and, hence, causing increased release of gas molecules per unit volume.

3.1.3 Effects of operating temperature

Using the same alkaline electrolyte, experiments were conducted to study the effects of electrolyte temperature on the generation of BNBs, keeping all the other parameters constant. Whilst the mean bubble diameter was not significantly affected by temperature, the results depicted in Figure 6 show that the bubble number density increases sharply with decreasing temperature. Gas release at the electrodes is a good example of nucleation which is driven by gas supersaturation. The continuous redox reactions on the electrodes lead to supersaturation of the liquid with gas, promoting the formation of gas bubbles. In a supersaturated system, however, homogeneous nucleation happens because of the electrolyte solution's attempt to re-establish its state of equilibrium by phase separation at a constant temperature.[42] The rate of supersaturation of liquid is driven by the rate of solubility of the electrolytic gases. Gas solubility being higher at low temperatures, increases the rate of supersaturation which, in turn, enhances the nucleation of gas bubbles.

3.1.4 Effects of electrolyte concentration

In this case, the electrolyte concentration of the alkaline KOH solution was varied within the range 0.05 – 100 mM, keeping other parameters constant. Again, there were little effects on the mean bubble diameter. The other effects on the generation of BNBs in the BES cell are depicted in Figure 7. The bubble number density increases exponentially as a function of alkaline electrolyte concentration, reaching 1.3×10^{8} bubble.mL^{-1} at 100 mM. At higher electrolyte concentrations, the ionic flux is more intense causing enhanced oxidation and reduction of electrolyte and leading to the formation of more gas molecules per unit volume.

3.1.5 Effects of applied voltage

Varying the voltage had little effect on the mean bubble diameter. Other effects depicted in Figure 8, show that increasing the applied voltage causes a sharp increase in the bubble number density which attains 8.9×10^{8} bubble.mL^{-1} at 25 V. A higher potential difference increases the electron flux, resulting in improved electrolysis, which enhances gas formation in the cell.

In conclusion, various combinations of electrolyte, electrolyte concentration, operating time, operating temperature and applied voltage will lead to different results. The above experiments have elucidated the effects of each operating parameter and can be used as a basis for optimising the generation of BNBs in a batch electrolysis cell.

3.2 Generation of BNBs in the continuous electrolysis system

Electrolysis was also studied using the CES configuration (Figure 2) operated for a period of 60 min. An alkaline electrolyte solution of 100 mM concentration and an operating temperature of 20 ˚C were used. The applied voltage was varied but the electrolyte flowrate through the cell was fixed of 1.85 $mL.min^{-1}$, giving a constant residence time of 390 s. The separation membrane allowed the hydrogen-filled BNBs released from the cathode and the oxygen-filled BNBs formed on the anode to be collected separately at the exit from the cell. The characteristics of the oxygen- and hydrogen-filled BNB suspensions, in terms of bubble size distribution, bubble number density, mean bubble diameter and zeta potential are presented in Figure 9 and Figure 10, respectively. The two different suspensions exhibit similar characteristics, although there are significantly more oxygen-filled BNBs produced than hydrogen-filled ones as the effect of applied voltage appears to be more pronounced in case of the former BNBs.

By virtue of stochiometric reaction in an alkaline electrolyte, the number of hydrogen molecules produced is twice the number of oxygen molecules. Thus, assuming that both oxidation and reduction occur at equal pressure and temperature, the volume of hydrogen gas produced is double that of oxygen gas. Despite this larger hydrogen gas volume, however, the much higher solubility of oxygen gas in water compared to that of hydrogen gas (26.875 times higher at standard pressure and temperature), leads to much more supersaturation of the electrolyte solution at the anode relative to the cathode and, hence, the nucleation of much greater number of oxygen BNBs than hydrogen BNBs.

A further potentially influential parameter is the hydraulic shear responsible for the efficient detachment of bubbles from the electrodes, because accumulation of bubbles reduces the efficiency of the redox reactions. The continuous flow of electrolyte solution exerts a shear stress which promotes bubble detachment. A detailed study would be required to determine the optimum operating conditions.

4 Conclusions

An electrolysis method for producing bulk nanobubble suspensions in water has been described. The technique has been demonstrated in aqueous alkaline, neutral and acidic electrolyte solutions. The method can be used in either an undivided electrolytic cell to generate a mixture of hydrogen- and oxygen-filled bulk nanobubble suspension or in a divided electrolytic cell, separating the anode and cathode compartments, to prepare separate suspensions of hydrogen- and oxygen-filled bulk nanobubbles. The operating parameters influence the effectiveness of BNB generation, but have little effect on the mean bubble size which is typically on the order of 100 nm. In this study, the BNB yield in water could be enhanced up to ~ 8×10^8 bubble.mL^{-1} by using a greater current input, longer operating time, higher electrolyte concentration or lower water operating temperature. The type of electrolyte is critical to the colloidal stability of the BNBs produced. BNBs formed in an alkaline electrolyte exist in a stable cluster form, but they dissociate into tiny primary stable nanobubbles on the order of 1 nm in neutral and acidic electrolytes, which is consistent with our previous findings on the clustering of BNBs.

Declaration of competing interest

There are no conflicts of interest to declare.

Acknowledgements

This work was supported by EPSRC Grant EP/L025108/1.

References

(1) ISO 20480-1:2017 https://www.iso.org/cms/render/live/en/sites/isoorg/contents/data/standard/06/81/68187.html (accessed 2021 -11 -09).

(2) Jadhav, A. J.; Ferraro, G.; Barigou, M. Generation of Bulk Nanobubbles Using a High-Shear Rotor–Stator Device. *Ind. Eng. Chem. Res.* **2021**, *60* (23), 8597–8606. https://doi.org/10.1021/acs.iecr.1c01233.

(3) Nirmalkar, N.; Pacek, A. W.; Barigou, M. On the Existence and Stability of Bulk Nanobubbles. *Langmuir* **2018**, *34* (37), 10964–10973. https://doi.org/10.1021/acs.langmuir.8b01163.

(4) Peyman, S. A.; McLaughlan, J. R.; Abou-Saleh, R. H.; Marston, G.; Johnson, B. R. G.; Freear, S.; Coletta, P. L.; Markham, A. F.; Evans, S. D. On-Chip Preparation of Nanoscale Contrast Agents towards High-Resolution Ultrasound Imaging. *Lab. Chip* **2016**, *16* (4), 679–687. https://doi.org/10.1039/C5LC01394A.

(5) Jadhav, A. J.; Barigou, M. Bulk Nanobubbles or Not Nanobubbles: That Is the Question. *Langmuir* **2020**, *36* (7), 1699–1708. https://doi.org/10.1021/acs.langmuir.9b03532.

(6) Jadhav, A. J.; Barigou, M. Proving and Interpreting the Spontaneous Formation of Bulk Nanobubbles in Aqueous Organic Solvent Solutions: Effects of Solvent Type and Content. *Soft Matter* **2020**, *16* (18), 4502–4511. https://doi.org/10.1039/D0SM00111B.

(7) Millare, J. C.; Basilia, B. A. Nanobubbles from Ethanol-Water Mixtures: Generation and Solute Effects via Solvent Replacement Method. *ChemistrySelect* **2018**, *3* (32), 9268–9275. https://doi.org/10.1002/slct.201801504.

(8) Millare, J. C.; Basilia, B. A. Dispersion and Electrokinetics of Scattered Objects in Ethanol-Water Mixtures. *Fluid Phase Equilibria* **2019**, *481*, 44–54. https://doi.org/10.1016/j.fluid.2018.10.013.

(9) Ohgaki, K.; Khanh, N. Q.; Joden, Y.; Tsuji, A.; Nakagawa, T. Physicochemical Approach to Nanobubble Solutions. *Chem. Eng. Sci.* **2010**, *65* (3), 1296–1300. https://doi.org/10.1016/j.ces.2009.10.003.

(10) Ushikubo, F. Y.; Furukawa, T.; Nakagawa, R.; Enari, M.; Makino, Y.; Kawagoe, Y.; Shiina, T.; Oshita, S. Evidence of the Existence and the Stability of Nano-Bubbles in Water. *Colloids Surf. Physicochem. Eng. Asp.* **2010**, *361* (1), 31–37. https://doi.org/10.1016/j.colsurfa.2010.03.005.

(11) Matsuki, N.; Ishikawa, T.; Ichiba, S.; Shiba, N.; Ujike, Y.; Yamaguchi, T. Oxygen Supersaturated Fluid Using Fine Micro/Nanobubbles. *Int. J. Nanomedicine* **2014**, *9* (1), 4495–4505. https://doi.org/10.2147/IJN.S68840.

(12) Liu, S.; Kawagoe, Y.; Makino, Y.; Oshita, S. Effects of Nanobubbles on the Physicochemical Properties of Water: The Basis for Peculiar Properties of Water Containing Nanobubbles. *Chem. Eng. Sci.* **2013**, *93*, 250–256. https://doi.org/10.1016/j.ces.2013.02.004.

(13) Matsuno, H.; Ohta, T.; Shundo, A.; Fukunaga, Y.; Tanaka, K. Simple Surface Treatment of Cell-Culture Scaffolds with Ultrafine Bubble Water. *Langmuir* **2014**, *30* (50), 15238–15243. https://doi.org/10.1021/la5035883.

(14) Nakatake, Y.; Kisu, S.; Shigyo, K.; Eguchi, T.; Watanabe, T. Effect of Nano Air-Bubbles Mixed into Gas Oil on Common-Rail Diesel Engine. *Energy* **2013**, *59*, 233–239. https://doi.org/10.1016/j.energy.2013.06.065.

(15) Ushida, A.; Hasegawa, T.; Nakajima, T.; Uchiyama, H.; Narumi, T. Drag Reduction Effect of Nanobubble Mixture Flows through Micro-Orifices and Capillaries. *Exp. Therm. Fluid Sci.* **2012**, *39*, 54–59. https://doi.org/10.1016/j.expthermflusci.2012.01.008.

(16) Ushida, A.; Hasegawa, T.; Takahashi, N.; Nakajima, T.; Murao, S.; Narumi, T.; Uchiyama, H. Effect of Mixed Nanobubble and Microbubble Liquids on the Washing Rate of Cloth in an Alternating Flow. *J. Surfactants Deterg.* **2012**, *15* (6), 695–702. https://doi.org/10.1007/s11743-012-1348-x.

(17) Ebina, K.; Shi, K.; Hirao, M.; Hashimoto, J.; Kawato, Y.; Kaneshiro, S.; Morimoto, T.; Koizumi, K.; Yoshikawa, H. Oxygen and Air Nanobubble Water Solution Promote the Growth of Plants, Fishes, and Mice. *PLOS ONE* **2013**, *8* (6), e65339. https://doi.org/10.1371/journal.pone.0065339.

(18) Calgaroto, S.; Wilberg, K. Q.; Rubio, J. On the Nanobubbles Interfacial Properties and Future Applications in Flotation. *Miner. Eng.* **2014**, *60*, 33–40. https://doi.org/10.1016/j.mineng.2014.02.002.

(19) IDEC Global : Ultrafine Bubble Generation Technology https://www.idec.com/home/finebubble/index.html (accessed 2021 -10 -09).

(20) OxyDoser™ PUREair http://www.oxydoser.com/oxydoser-pureair.html (accessed 2021 -10 -09).

(21) Fine Bubble OK Brand Generators https://www.finebubble-ok.com/ (accessed 2021 -10 -09).

(22) Yasuda, K.; Matsushima, H.; Asakura, Y. Generation and Reduction of Bulk Nanobubbles by Ultrasonic Irradiation. *Chem. Eng. Sci.* **2019**, *195*, 455–461. https://doi.org/10.1016/j.ces.2018.09.044.

(23) Nirmalkar, N.; Pacek, A. W.; Barigou, M. Bulk Nanobubbles from Acoustically Cavitated Aqueous Organic Solvent Mixtures. *Langmuir* **2019**, *35* (6), 2188–2195. https://doi.org/10.1021/acs.langmuir.8b03113.

(24) Wang, Q.; Zhao, H.; Qi, N.; Qin, Y.; Zhang, X.; Li, Y. Generation and Stability of Size-Adjustable Bulk Nanobubbles Based on Periodic Pressure Change. *Sci. Rep.* **2019**, *9* (1), 1118. https://doi.org/10.1038/s41598-018-38066-5.

(25) Ferraro, G.; J. Jadhav, A.; Barigou, M. A Henry's Law Method for Generating Bulk Nanobubbles. *Nanoscale* **2020**, *12* (29), 15869–15879. https://doi.org/10.1039/D0NR03332D.

(26) Kukizaki, M.; Goto, M. Size Control of Nanobubbles Generated from Shirasu-Porous-Glass (SPG) Membranes. *J. Membr. Sci.* **2006**, *281* (1), 386–396. https://doi.org/10.1016/j.memsci.2006.04.007.

(27) Kukizaki, M. Microbubble Formation Using Asymmetric Shirasu Porous Glass (SPG) Membranes and Porous Ceramic Membranes—A Comparative Study. *Colloids Surf. Physicochem. Eng. Asp.* **2009**, *340* (1), 20–32. https://doi.org/10.1016/j.colsurfa.2009.02.033.

(28) Ahmed, A. K. A.; Sun, C.; Hua, L.; Zhang, Z.; Zhang, Y.; Zhang, W.; Marhaba, T. Generation of Nanobubbles by Ceramic Membrane Filters: The Dependence of Bubble Size and Zeta Potential on Surface Coating, Pore Size and Injected Gas Pressure. *Chemosphere* **2018**, *203*, 327–335. https://doi.org/10.1016/j.chemosphere.2018.03.157.

(29) Oh, S. H.; Han, J. G.; Kim, J.-M. Long-Term Stability of Hydrogen Nanobubble Fuel. *Fuel* **2015**, *158*, 399–404. https://doi.org/10.1016/j.fuel.2015.05.072.

(30) Shiva Kumar, S.; Himabindu, V. Hydrogen Production by PEM Water Electrolysis – A Review. *Mater. Sci. Energy Technol.* **2019**, *2* (3), 442–454. https://doi.org/10.1016/j.mset.2019.03.002.

(31) Seddon, J. R. T.; Lohse, D.; Ducker, W. A.; Craig, V. S. J. A Deliberation on Nanobubbles at Surfaces and in Bulk. *ChemPhysChem* **2012**, *13* (8), 2179–2187. https://doi.org/10.1002/cphc.201100900.

(32) Kikuchi, K.; Ioka, A.; Oku, T.; Tanaka, Y.; Saihara, Y.; Ogumi, Z. Concentration Determination of Oxygen Nanobubbles in Electrolyzed Water. *J. Colloid Interface Sci.* **2009**, *329* (2), 306–309. https://doi.org/10.1016/j.jcis.2008.10.009.

(33) Kikuchi, K.; Tanaka, Y.; Saihara, Y.; Maeda, M.; Kawamura, M.; Ogumi, Z. Concentration of Hydrogen Nanobubbles in Electrolyzed Water. *J. Colloid Interface Sci.* **2006**, *298* (2), 914–919. https://doi.org/10.1016/j.jcis.2006.01.010.

(34) Wu, Z.; Chen, H.; Dong, Y.; Mao, H.; Sun, J.; Chen, S.; Craig, V. S. J.; Hu, J. Cleaning Using Nanobubbles: Defouling by Electrochemical Generation of Bubbles. *J. Colloid Interface Sci.* **2008**, *328* (1), 10–14. https://doi.org/10.1016/j.jcis.2008.08.064.

(35) Zhang, L.; Zhang, Y.; Zhang, X.; Li, Z.; Shen, G.; Ye, M.; Fan, C.; Fang, H.; Hu, J. Electrochemically Controlled Formation and Growth of Hydrogen Nanobubbles. *Langmuir* **2006**, *22* (19), 8109–8113. https://doi.org/10.1021/la060859f.

(36) C-Tech Leading Electro-Heating and Electrochemical Equipment https://www.ctechinnovation.com/ (accessed 2021 -10 -09).

(37) Nirmalkar, N.; Pacek, A. W.; Barigou, M. Interpreting the Interfacial and Colloidal Stability of Bulk Nanobubbles. *Soft Matter* **2018**, *14* (47), 9643–9656. https://doi.org/10.1039/C8SM01949E.

(38) Jadhav, A. J.; Barigou, M. On the Clustering of Bulk Nanobubbles and Their Colloidal Stability. *J. Colloid Interface Sci.* **2021**, *601*, 816–824. https://doi.org/10.1016/j.jcis.2021.05.154.

(39) Filipe, V.; Hawe, A.; Jiskoot, W. Critical Evaluation of Nanoparticle Tracking Analysis (NTA) by NanoSight for the Measurement of Nanoparticles and Protein Aggregates. *Pharm. Res.* **2010**, *27* (5), 796–810. https://doi.org/10.1007/s11095-010-0073-2.

(40) Zetasizer Nano ZSP | Expert Colloid & Protein Characterization - Product support| Malvern Panalytical https://www.malvernpanalytical.com/en/support/product-support/zetasizer-range/zetasizer-nano-range/zetasizer-nano-zsp (accessed 2021 -05 -17).

(41) Berne, B. J.; Pecora, R. *Dynamic Light Scattering: With Applications to Chemistry, Biology, and Physics*; Dover Publications, 2000.

(42) Vachaparambil, K. J.; Einarsrud, K. E. Explanation of Bubble Nucleation Mechanisms: A Gradient Theory Approach. *J. Electrochem. Soc.* **2018**, *165* (10), E504. https://doi.org/10.1149/2.1031810jes.

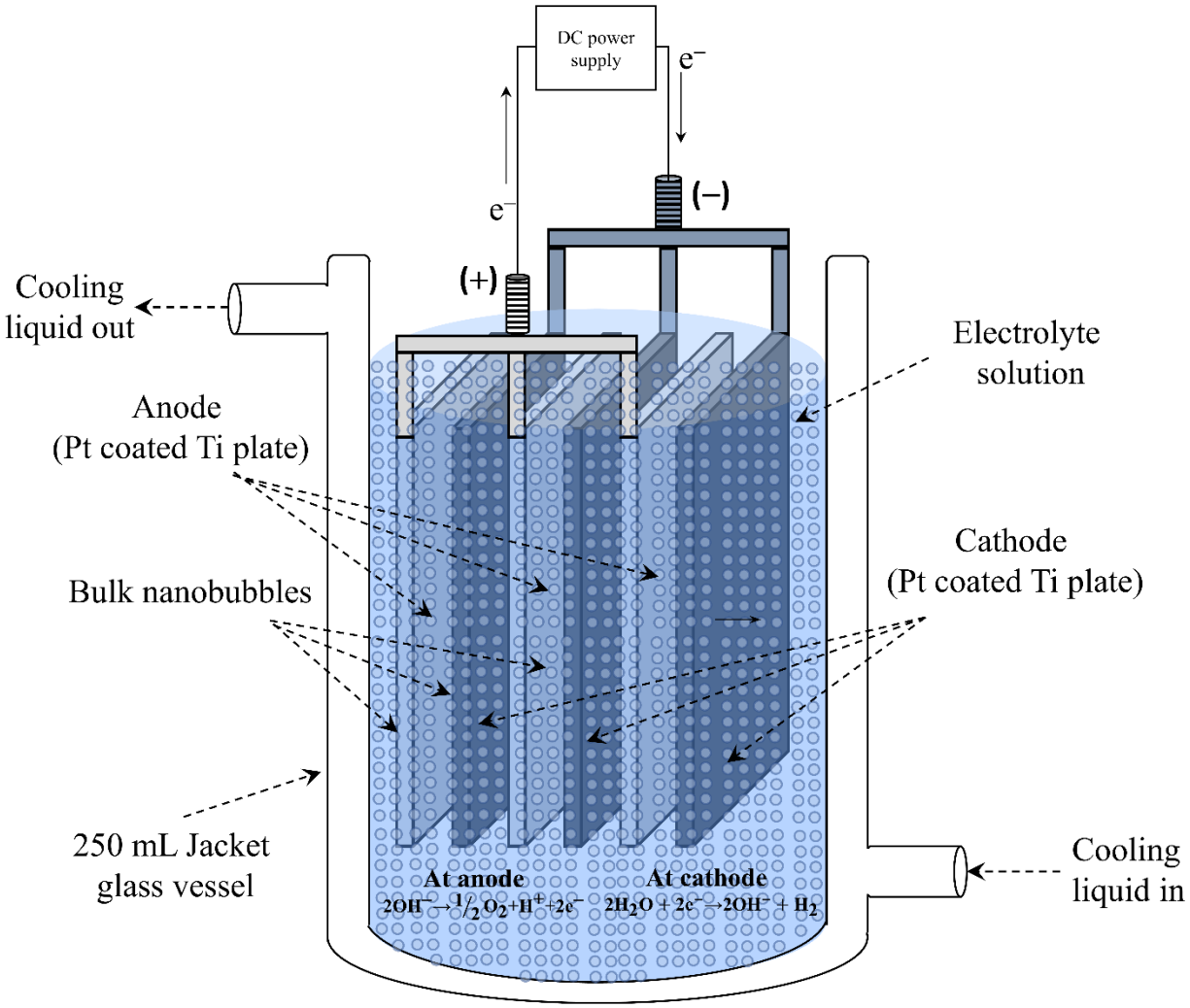

Figure 1. Schematic representation of BNB generation process in temperature-controlled batch electrolysis system (BES): example redox reactions shown are for an alkaline electrolyte solution.

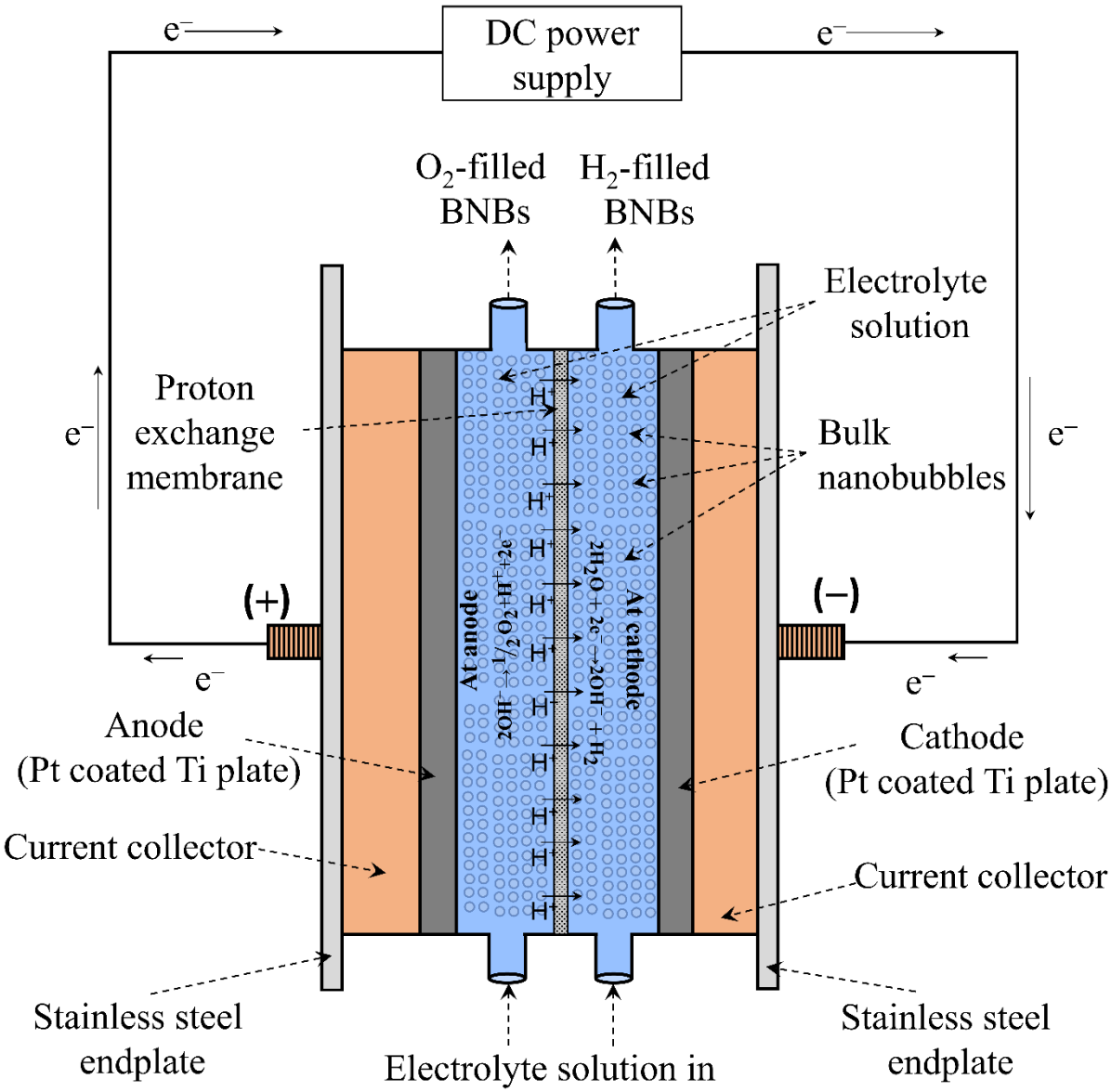

Figure 2. Schematic representation of BNB generation process in continuous electrolysis system (CES): example redox reactions shown are for an alkaline electrolyte solution.

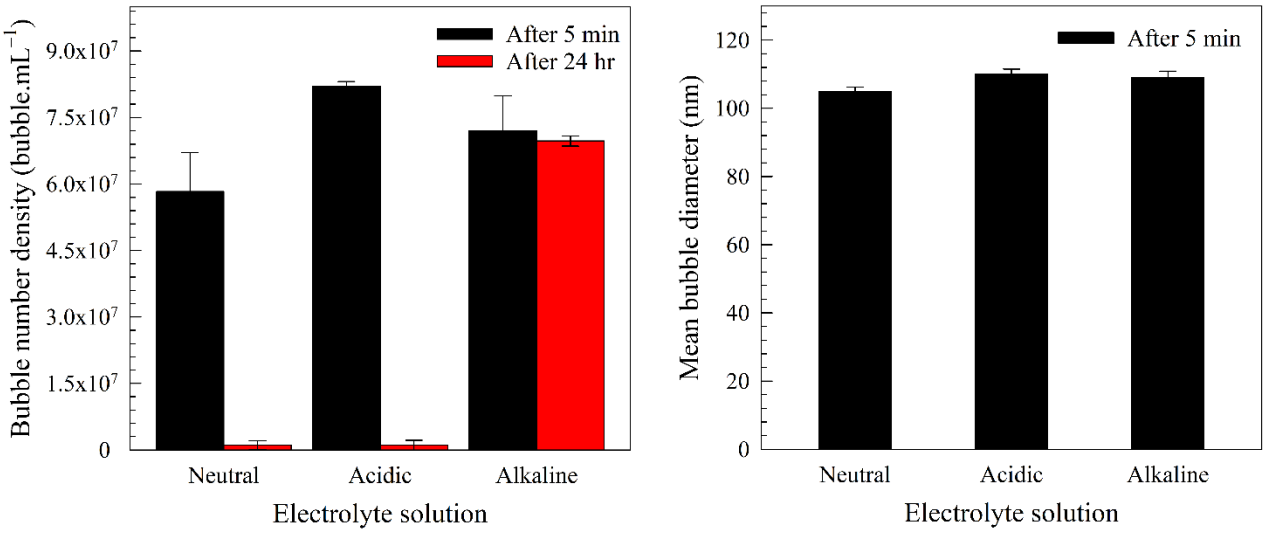

Figure 3. Generation of BNBs in different electrolyte solutions using the BES cell (NTA analysis): E_c = 10 mM, ΔV = 10 V, t = 60 min, T = 20 ºC.

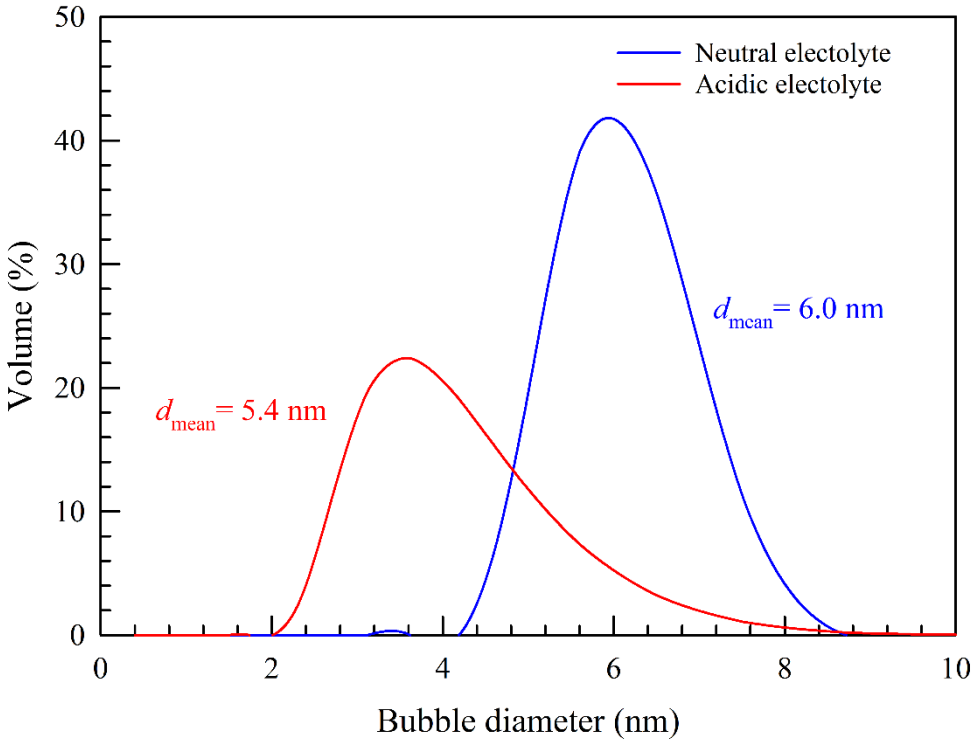

Figure 4. Bubble size distribution after 24 hr of neutral and acidic electrolyte BNB suspensions obtained in the BES cell (DLS analysis).

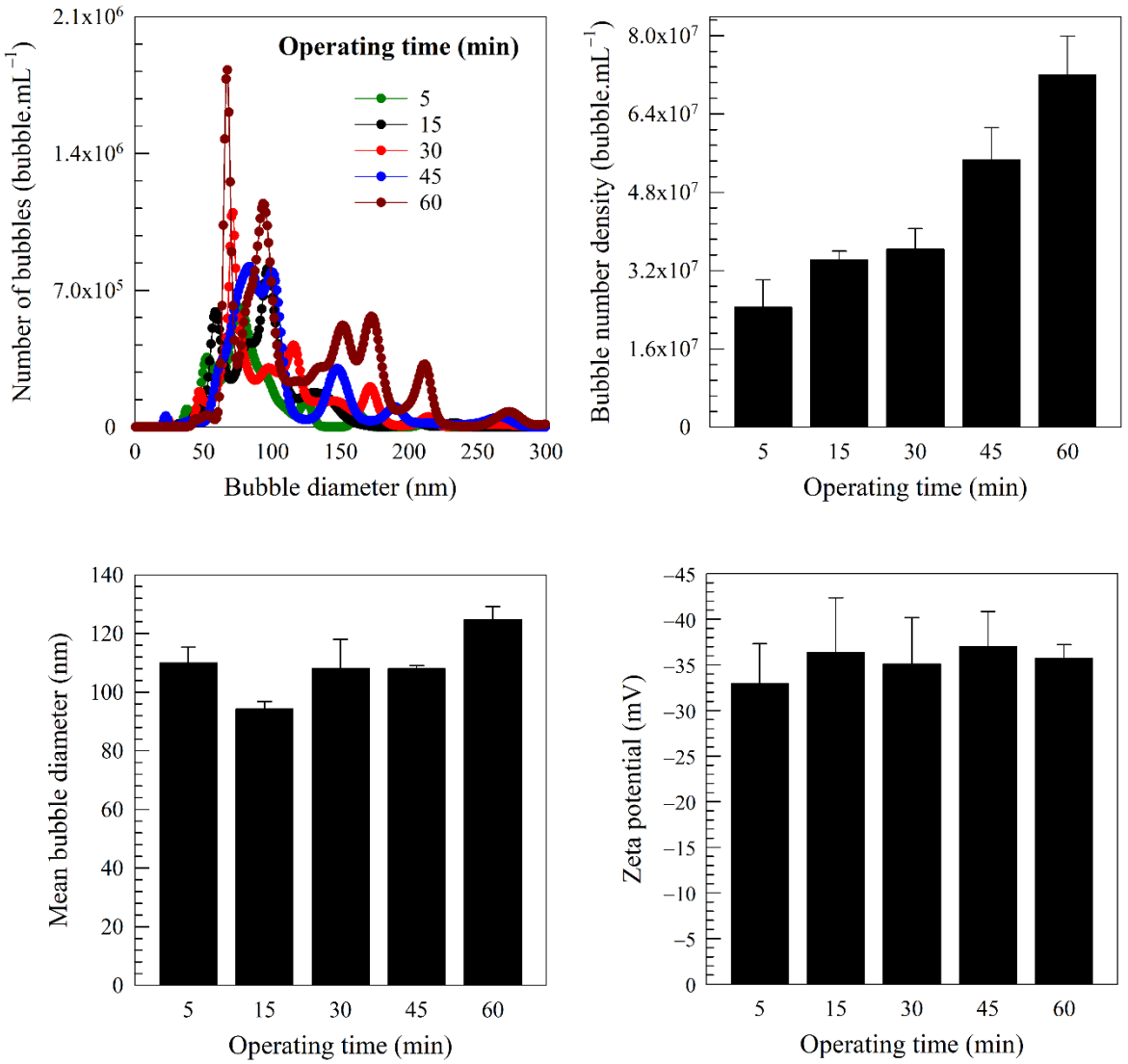

Figure 5. Effects of operating time on generation of BNBs in aqueous KOH solution using the BES cell: E_c = 10 mM, ΔV = 10 V, T = 20 ºC.

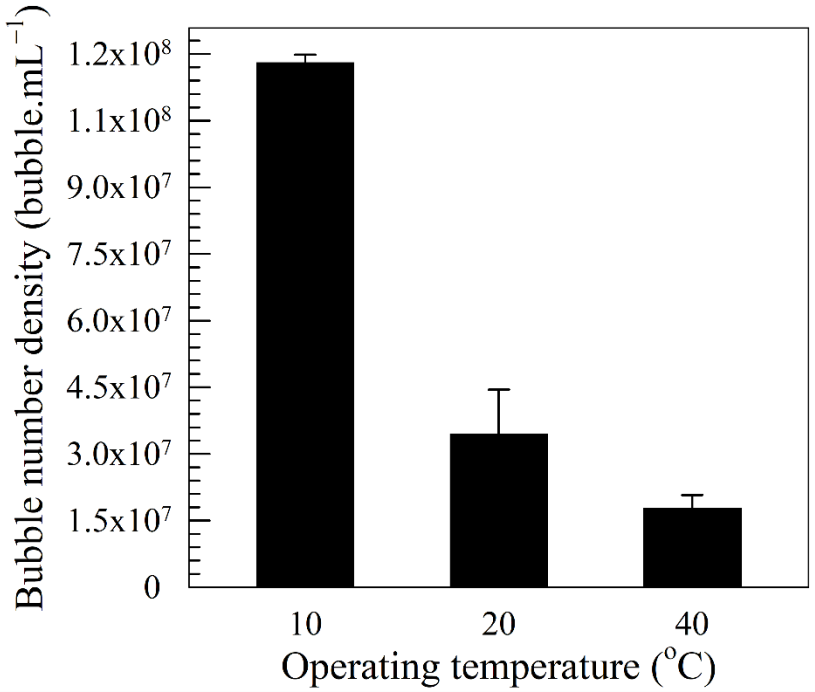

Figure 6. Effects of operating temperature on generation of BNBs in aqueous KOH solution using the BES cell: E_c = 10 mM, t = 60 min, ΔV = 10 V.

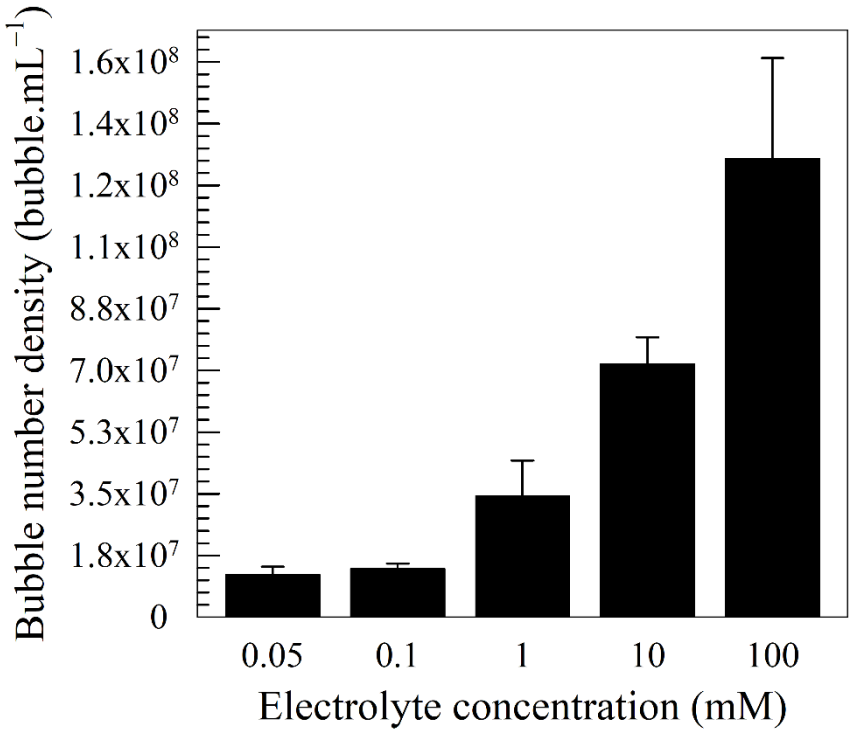

Figure 7. Effects of electrolyte concentration on generation of BNBs in aqueous KOH solution using the BES cell: t = 60 min, ΔV = 10 V, T = 20 ºC.

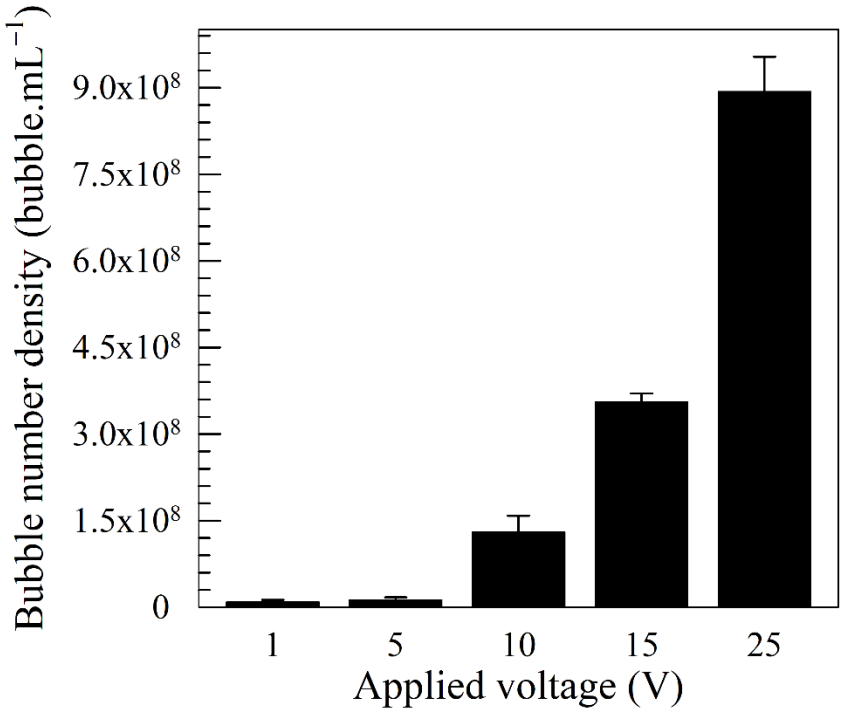

Figure 8. Effects of applied voltage on generation of BNBs in aqueous KOH solution using the BES cell: E_c = 100 mM, t = 60 min, T = 20 ºC.

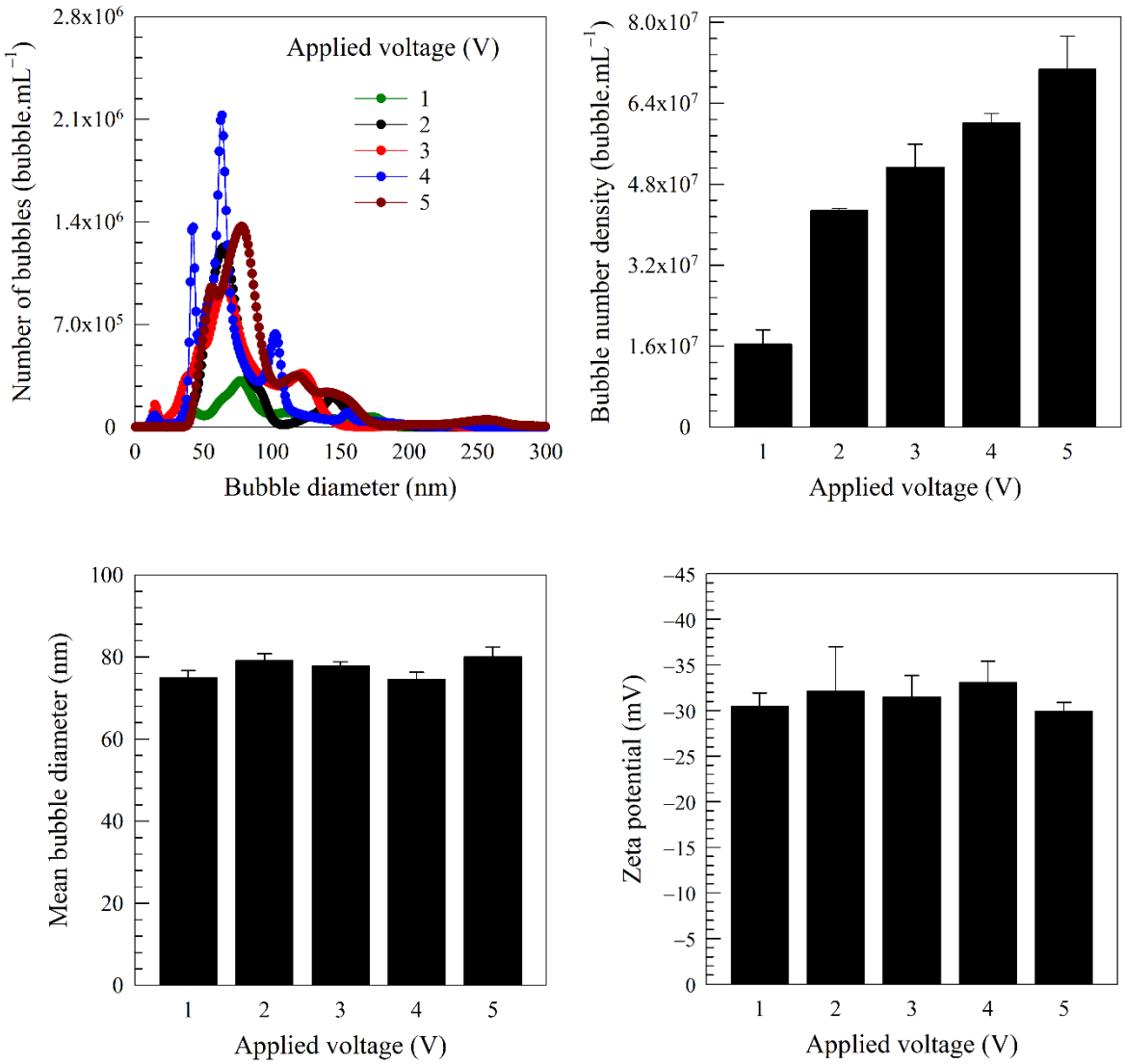

Figure 9. Characteristics of oxygen-filled BNB suspensions produced in aqueous KOH solution using the CES configuration at different applied voltages: E_c = 100 mM, t = 60 min, T = 20 ºC.

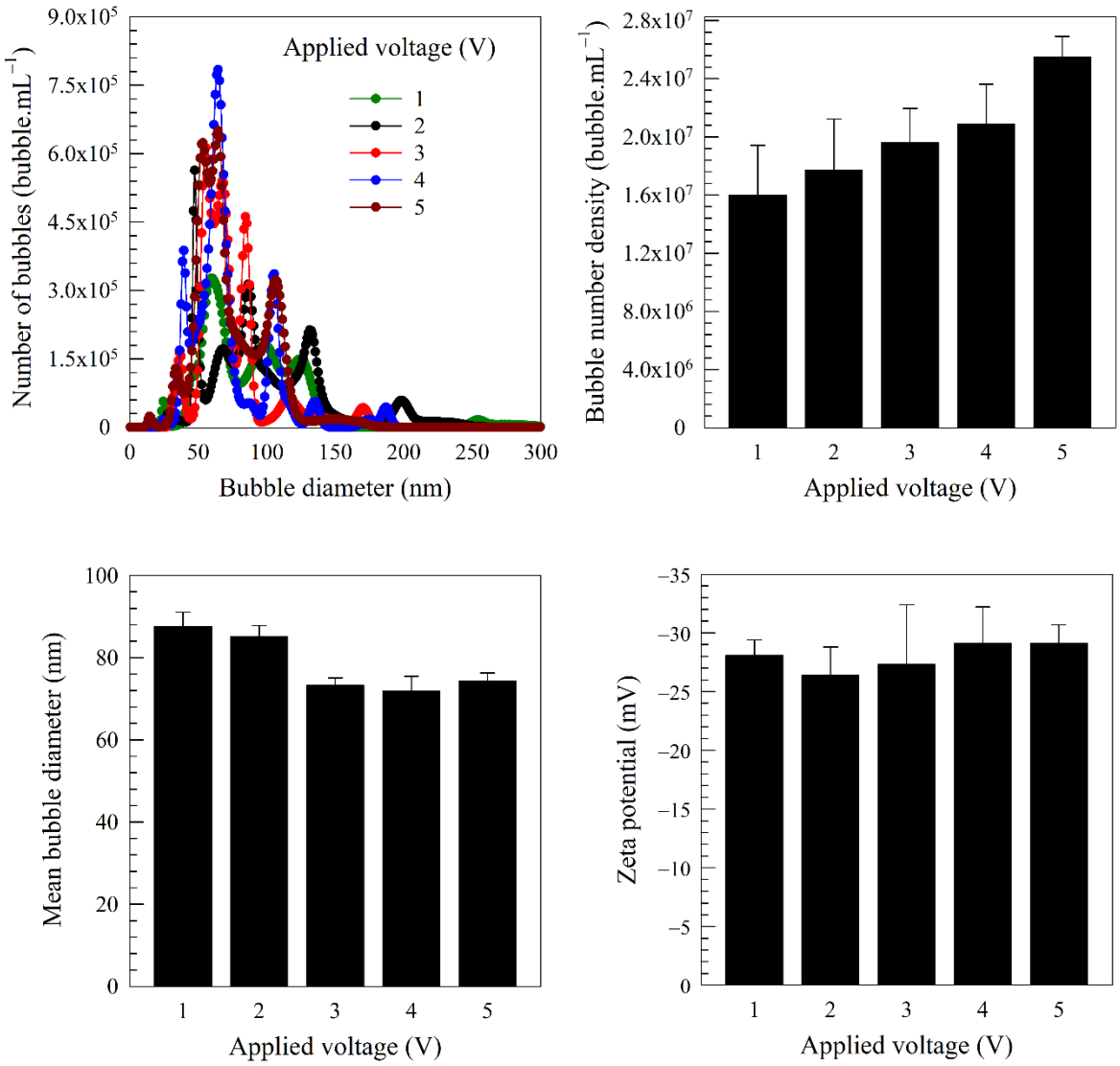

Figure 10. Characteristics of hydrogen-filled BNB suspensions produced in aqueous KOH solution using the CES configuration at different applied voltages: E_c = 100 mM, t = 60 min, T = 20 ºC.

For Table of Contents Only